Proc. Natl. Acad. Sci. USA
Vol. 84, pp. 8385–8389, December 1987
Biochemistry

A bifurcated hydrogen-bonded conformation in the d(A·T) base pairs of the DNA dodecamer d(CGCAAATTTGCG) and its complex with distamycin

[P-DNA/antitumor drug/poly(dA)·poly(dT)/DNA bending/propeller-twisted base pairs]

MIQUEL COLL, CHRISTIN A. FREDERICK, ANDREW H.-J. WANG, AND ALEXANDER RICH

Department of Biology, Massachusetts Institute of Technology, Cambridge, MA 02139

Contributed by Alexander Rich, August 21, 1987

ABSTRACT **The crystal structures of d(CGCA$_3$T$_3$GCG) complex to the antitumor drug distamycin and the DNA fragment alone were solved by x-ray diffraction at 2.2 and 2.5 Å resolution, respectively. The drug lies in the narrow minor groove near the center of the B-DNA fragment covering 5 of the 6 A·T base pairs. It is bound to the DNA by hydrogen bonding, van der Waals, and electrostatic interactions. In addition, the DNA was found to have an unusual conformation in the (dA)$_3$·(dT)$_3$ regions. These base pairs have a high positive propeller twist so that in the major groove the adenine amino group is located intermediate between the carbonyl O-4 groups of two adjacent thymines of the opposite strand, making bifurcated hydrogen bonds to the two thymine residues. This suggests a model to explain the unusual properties of poly(dA)·poly(dT) in which a modified B conformation is associated with a large propeller twist of the bases and a set of continuous bifurcating hydrogen bonds along the major groove, which may provide incremental stability to these segments. In addition, shorter segments of (dA)$_{3-6}$·(dT)$_{3-6}$ may have this conformation in the midst of B-DNA and stabilize bends in the DNA that may be associated with stacking on one of the high propeller-twisted bases at the ends of these segments.**

During the past decade, our awareness of the conformational potentials of DNA has broadened substantially. The general outline of the DNA double helix has remained in place, but the detailed look afforded by single crystal x-ray diffraction analysis has revealed a variety of conformational changes, most of which are related to differences in DNA composition as well as sequence. The antitumor drugs netropsin and distamycin are believed to bind to DNA in the minor groove at A+T-rich sequences (1). The mode of interaction of netropsin with DNA has been demonstrated by the structure of netropsin bound to a dodecamer of DNA containing 4 A·T base pairs (2). In that case, the A·T base pair segment of the B-DNA dodecamer has a narrow minor groove into which the elongated netropsin molecule can fit. We have extended this study by using the dodecamer d(CGCA$_3$T$_3$GCG), which has been crystallized by itself as well as cocrystallized with a longer groove-binding molecule, distamycin. The mode of binding of distamycin to DNA is similar in many ways to that of netropsin, but with a longer binding region. In addition, the DNA itself has a distinct structural modification. The A·T base pairs have a general tendency toward a large propeller twist, such that the amino group of 1 base pair, in addition to being hydrogen-bonded to the O-4 of the opposite thymine, is also within hydrogen-bonding distance to the O-4 of the adjacent thymine 1 base pair removed. The amino group is thus in a position to form a bifurcated hydrogen bond to two thymines on the opposite strand. This conformation, found in the DNA molecule with or without the complexed drug, provides a model that may explain the unusual properties of poly(dA)·poly(dT) (3–7). The propeller twist stabilized by bifurcating hydrogen bonds may also provide some understanding of the mechanism of DNA bending.

The publication costs of this article were defrayed in part by page charge payment. This article must therefore be hereby marked "*advertisement*" in accordance with 18 U.S.C. §1734 solely to indicate this fact.

MATERIALS AND METHODS

The DNA dodecamer was synthesized by the phosphate triester method and purified by HPLC to >95%. The complex crystal was prepared from a solution containing 1.0 mM DNA dodecamer, 20 mM sodium cacodylate (pH 6.5), 8 mM $MgCl_2$, 1.0 mM spermine, 1.1 mM distamycin (Boehringer Mannheim) and 10% (vol/vol) 2-methyl-2,4-pentanediol (2-MPD) using vapor diffusion against a 50% 2-MPD reservoir at room temperature. An attempt was also made under similar conditions to crystallize this DNA sequence alone and with another synthetic groove-binding molecule, SN7167, provided by W. Denny (Cancer Research Institute of New Zealand). DNA crystals formed in both of these cases. In the latter case, well-formed yellow single crystals were found in the medium, but no ordered drug could be seen in the crystal lattice after the structure was solved. The unit cell dimensions for the dodecamer–distamycin complex crystal were a = 25.20, b = 41.07, and c = 64.65 Å with the space group $P2_12_12_1$. Three-dimensional diffraction data were collected at 15°C using a Nicolet P3 diffractometer to a resolution of 2.2 Å with 2369 observed reflections with an intensity $>2\sigma(F)$. The crystals of the DNA alone had cell unit dimensions a = 25.20, b = 41.65, and c = 65.81 Å. X-ray data were collected to a resolution of 2.5 Å yielding 1728 reflections at the $2\sigma(F)$ level.

The overall similarity of these unit cell dimensions with the published dimensions of d(CGCGAATTCGCG) (8) suggested a similar lattice. Accordingly, the coordinates of that dodecamer, with appropriate changes in the central 6 base pairs, were used as a starting point in the refinement of both structures using the Konnert and Hendrickson constrained least-squares refinement procedure (9). Initial refinement was carried out on the complex crystal by excluding the drug to an initial R factor of 30%. At that stage, the first Fourier map already showed the drug lying in the minor groove. Up to 38 water molecules were then added gradually to improve the phasing, reducing the R factor to 26%. A difference Fourier map was then displayed on an Evans and Sutherland PS340 and the program FRODO (10) was used to fit the drug in the electron density observed within the minor groove of the DNA (Fig. 1). Distamycin consists of three pyrrolamide groups attached in a linear array with a formamide group at one end and a propylamidinium group at the other end. Thus, the molecule is asymmetric and it could potentially be fitted into the difference Fourier map in two orientations. It was apparent that one fit was much better than the other (Fig. 1). Refinement was continued with the inclusion of the drug and

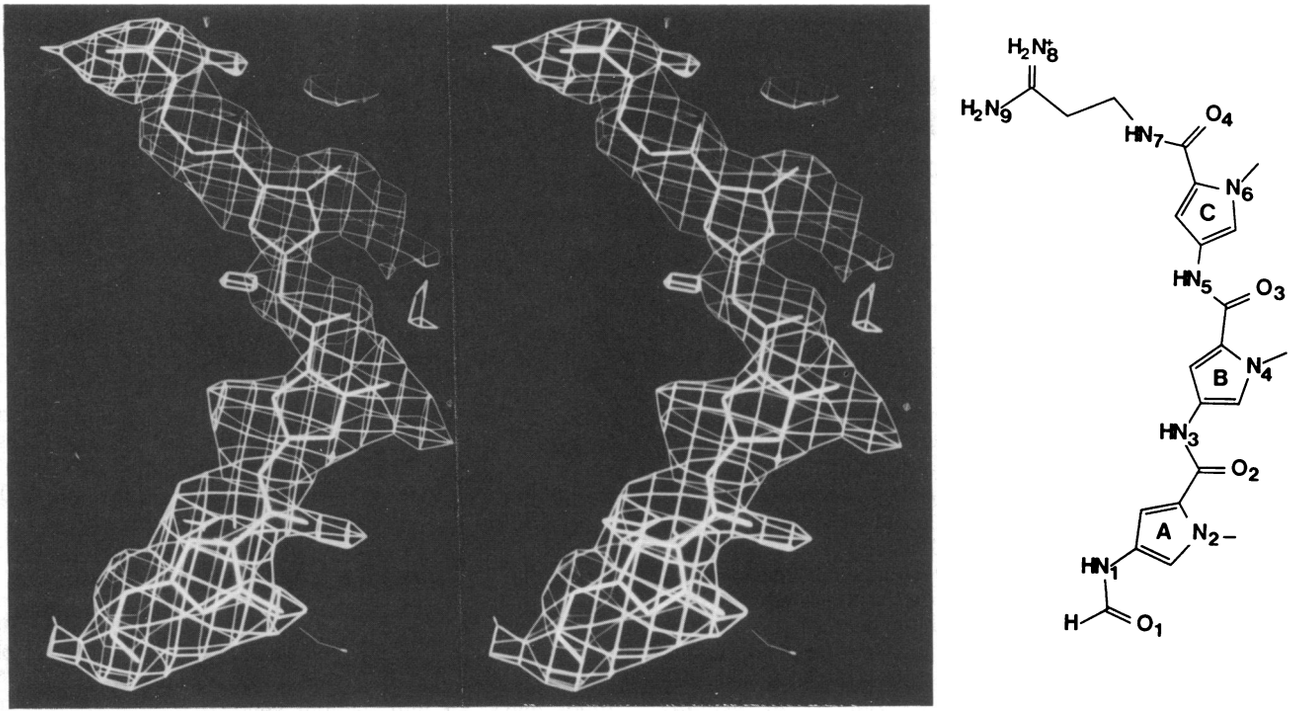

FIG. 1. (*Left*) A stereo drawing of a difference Fourier (Fo-Fc) map of a portion of the minor groove of the DNA duplex showing the region occupied by the distamycin molecule. (*Right*) Structure of the distamycin in approximately the same orientation as that shown in the difference Fourier map. Distamycin has an arc-like conformation and careful inspection shows that the molecule is not flat but has a slight continuous twist.

the addition of more solvent molecules up to 70 with a final *R* factor of 19.6% for the 2.2-Å data. No constraint was put on the distance between the DNA and the drug except in the late stages of refinement once the drug had already established hydrogen-bonding distances. No torsional angle constraints were imposed on the drug or the DNA. Only weak hydrogen-bonding constraints were used for the Watson–Crick base pairs in the DNA. In the DNA structure without the drug, the final *R* factor was 16% at 2.5 Å with 32 water molecules. The refined coordinates of both the DNA–distamycin complex and the DNA alone will be deposited in the Brookhaven Protein Data Bank.

RESULTS

Interactions between Distamycin and DNA. Fig. 2 shows stereoscopic views of both skeletal and van der Waals representations (oriented 90° apart) of the DNA–distamycin complex. The three pyrrole rings in the distamycin A have a slight twist, so that the molecule is not planar. There is an angle of 15° between the plane of pyrrole rings A and B and 11° between B and C. The planar amides link the pyrrole rings such that the molecule has a crescent shape, which is approximately complementary to the natural curvature of the minor groove of B-DNA as clearly shown in Fig. 2*A*. In the van der Waals diagram (Fig. 2*B*), the drug fully occupies the minor groove of the DNA in the central A·T segment, with complete van der Waals contact between the walls and floor of the minor groove and the drug molecule. There is no room for any solvent molecule to be interposed between the distamycin and the DNA. The oxygen atoms of the amide linkages are pointing away from the DNA groove, and solvent water molecules are found within hydrogen-bonding distances.

Detailed interactions between distamycin and the minor groove of the double helix are illustrated diagramatically in Fig. 3. The four amide nitrogens N-1–N-7 plus the propylamidinium nitrogen atom N-9 are all on the same side of the distamycin A, facing the minor groove (Fig. 1). It can be seen that N-1, N-5, and N-7 form bifurcated hydrogen bonds simultaneously to both an adenine N-3 and a thymine O-2 atom, somewhat similar to those found in the netropsin complex (2) except that these appear to be more symmetrical and the distances are nearly equivalent. However, the amide N-3 is 4.4 and 3.9 Å away from its potential hydrogen bond acceptors. This reflects the fact that the periodicity of the pyrrolamide unit is not integrally related to the periodicity of the hydrogen bonding acceptors on the floor of the minor groove of the double helix. In the region immediately beyond N-1, a water molecule is found that hydrogen bonds to both the O-2 of thymine on one side and to the N-3 of adenine on the other. This is part of the spine of hydration, which has been observed in the minor groove of d(CGCGAATTCGCG) dodecamer crystals (8). The nitrogen N-9 in the propylamidinium group forms only one hydrogen bond to the N-3 of A-4. The other hydrogen of N-9 is bound to the O-3′ hydroxyl terminal of a symmetry-related DNA molecule.

Conformation of the DNA. In the drug–DNA complex, there is a large positive propeller twist in the A_3T_3 segments of the molecule. Whereas the propeller twist in the 6 C·G base pairs averages 14°, the A·T base pairs average 20°. The base pairs A-6–T-19 and T-9–A16 have positive twists of 21° and 26°, respectively. In the starting model, the average propeller twist of the A·T base pairs was 17°. Thus, with the additional 2 A·T base pairs forming an AAATTT segment, there was a significant increase in the propeller twist. The effect of the propeller twist is shown in Fig. 4. The amino group of A-5 is almost midway between the carbonyl O-4 of T-20 (2.9 Å) and O-4 of T-19 (2.7 Å). The geometry is typical of a bifurcated hydrogen bond. Similar short distances are seen with other groups that have a potential for bifurcating hydrogen-bond interactions, including N-6 of A-4 with O-4 of T-20 (3.2 Å), N-6 of A-16 with O-4 of T-8 (3.0 Å), and N-4 of C-3 with O-4 of T-21 (3.2 Å). These are shown in the skeletal diagram of Fig. 2*A* by the diagonal lines drawn between base pairs in the major groove.

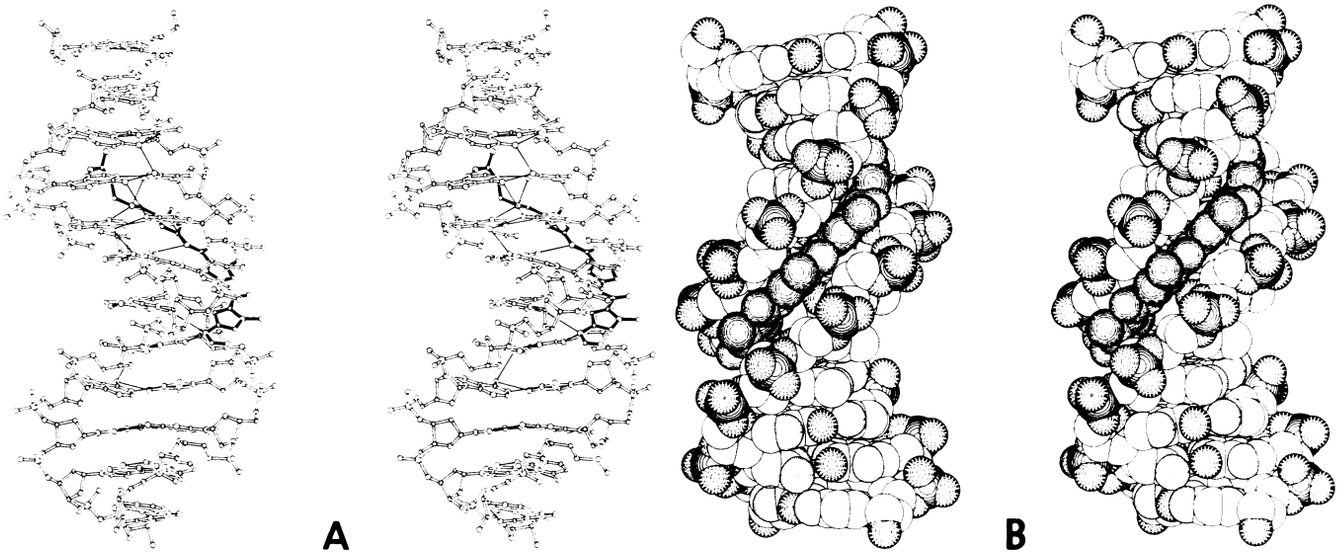

FIG. 2. Stereo diagrams of the complex of the DNA dodecamer and distamycin. (*A*) Skeletal diagram: the bonds of distamycin are solid, whereas those of the DNA are open. The distamycin molecule can be seen wrapping around the side and continuing onto the back of the DNA helix. The bifurcated hydrogen bonds that connect the drug molecule to the narrow minor groove are shown as thin lines. Likewise, the bifurcated interactions in the major groove due to the propeller twisting of the base pairs are also drawn as thin lines. The propeller twisting of the base pairs is readily evident in the skeletal diagram. (*B*) van der Waals diagram: the complex is rotated 90° relative to *A*. All atoms of distamycin are shaded with heavy black circles, whereas in DNA, nitrogens are drawn as dotted spheres, oxygens as dashed spheres, phosphorus as concentric circles, and carbons are unshaded.

In the 6 A·T base-pair region of this structure, four adenines are in positions that may involve bifurcated hydrogen bonds, suggesting that this may be an inherent feature of this type of molecule. Recently, Nelson *et al.* (11) have shown that the structure of d(CGCA$_6$GCG)·d(CGCT$_6$GCG) revealed a similar type of large propeller twisting with a geometry that predisposed the formation of bifurcated hydrogen bonds for all six A·T base pairs. This geometry may suggest an explanation for the unusual properties associated with poly(dA)·poly(dT) (3–7). To test this proposal, we have used the conformation of the segment A-5–A-6·T-19–T-20, shown in Fig. 4, as the asymmetric unit to build a double helix. The proposed structure is shown in a stereo diagram in Fig. 5. This helix has 10 base pairs per turn with a narrow minor groove. At the floor of the major groove is a zigzag array of bifurcating hydrogen bonds leading from one adenine N-6 to the carbonyl O-4 of the Watson–Crick base-paired

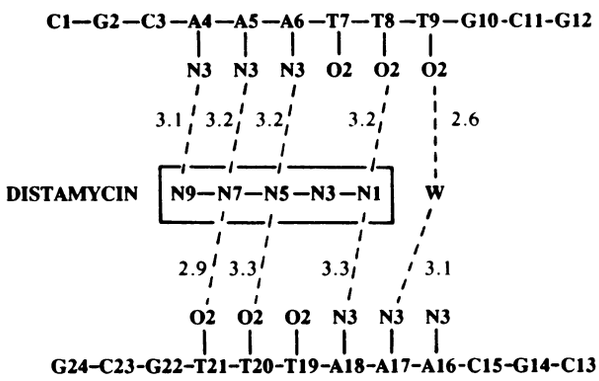

FIG. 3. A schematic diagram illustrating the hydrogen bonding between distamycin (box) and the electronegative nitrogen and oxygen atoms in the floor of the minor groove. Dashed lines indicate hydrogen bonding interactions and numbers indicate the length in Å of the hydrogen bonds. W, water of hydration found in the minor groove. The numbering system for the DNA molecule is shown here.

thymine as well as to the next O-4 of the thymine on the 5′ side in the pyrimidine strand.

To assess the influence of the drug on this conformation, we have also analyzed the structure of the same dodecamer in the absence of the drug. A similar trend toward high propeller twist was observed in the A·T region with some individual values greater than 25°. The N-6 amino nitrogen of A-16 and A-5 are close enough (both 3.2 Å) to carbonyl O-4 of T-8 and T-19, respectively, to be forming bifurcated hydrogen bonds. The fact that this favorable arrangement is present in two different loci of the A·T track suggests that this is an intrinsic property of the A·T sequences, which have a tendency to adopt the altered conformation. In solution, a series of similar conformations may exist in equilibrium, in different regions of A+T-rich sequences.

DISCUSSION

Distamycin Binding to DNA. The binding specificity of the antibiotic distamycin for A+T-rich regions in DNA can be explained in two ways: first, A·T base pairs are associated with a narrow minor groove and hence are tighter fitting to the elongated distamycin molecule; second, the presence of the amino group N-2 of guanine serves as a major steric block preventing the pyrrolamide chain from docking fully to the floor of the minor groove in G+C-rich segments. In this structure, the distamycin replaces the spine of hydration. The hydrogen bonding stabilization is enhanced by hydrophobic van der Waals contacts between the aromatic pyrrole rings of the drug and the walls of the minor groove. Because van der Waals interactions are proportional to the inverse sixth power of the distances, small changes in conformation will have a large effect on stability. Therefore, the narrowed minor groove is needed to give a large interacting van der Waals surface. The propylamidinium group provides a generalized electrostatic stabilization between the negatively charged nucleic acid and the positively charged drug. It has been shown that the center of the minor groove floor in the A·T region has the most positive electric potential (13), which is consistent with these observations. The binding of dis-

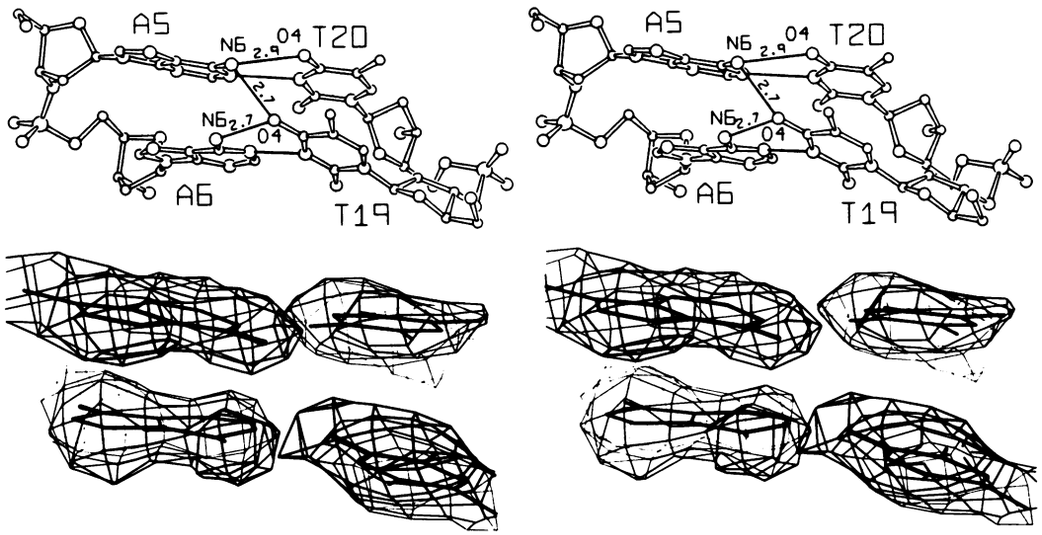

FIG. 4. Stereo diagrams (*Upper*) illustrating the bifurcated hydrogen bonding associated with the strong propeller twisting of A-5–A-6·T-19–T-20 with their hydrogen-bonding distances indicated. The electron density map (*Lower*) shows the manner in which the base pairs are propeller twisted. The upper diagram has been rotated slightly relative to the electron density map to display the hydrogen bond lengths more clearly.

tamycin and netropsin to DNA is similar but not identical. Both fit into narrowed minor grooves and have bifurcated hydrogen bonding, but there are some significant differences that are undoubtedly associated with the fact that the geometry of the molecules differ, both due to the additional pyrrole amide group in distamycin and to the fact that the terminal residues are different. Distamycin covers 5 of the 6 A·T base pairs, whereas netropsin covers 4 A·T base pairs (2). Footprinting experiments have yielded similar results (14). In view of these differences, it is reasonable to anticipate that they would have several closely related binding sites. NMR studies of the interaction of this type of drug with a variety of oligonucleotides have clearly revealed that the drugs can interact with the DNA in more than one manner (15, 16). The results have been interpreted as indicating that there is a dynamic flip-flop binding of drug to the DNA on the NMR time scale, consistent with the microheterogeneity of binding described here.

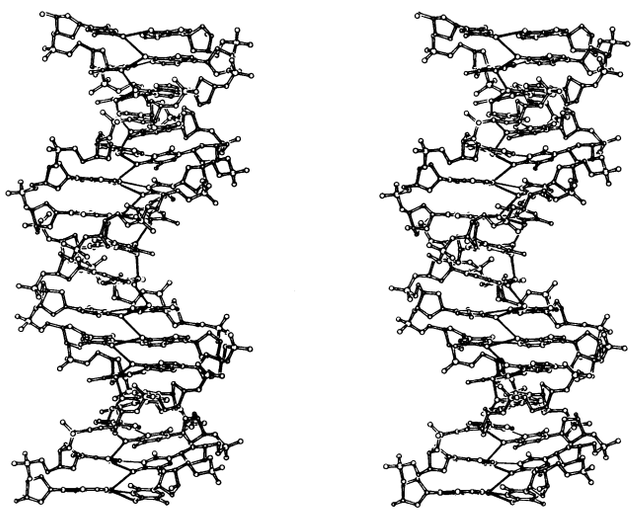

FIG. 5. Stereo diagram showing a model for poly(dA)·poly(dT) or P-DNA constructed from the bifurcated hydrogen bonding shown in Fig. 4 and extended into a double helix of 10 base pairs per turn. Solid line shows the bifurcating hydrogen bonding. Notice that in the minor groove the adenine H-2 proton is closest to the thymine H-1′ proton (average, 3.40 Å) of the thymidine sugar preceding the base-paired thymine residue on the 3′ side. This agrees well with the NMR data (12).

An Altered DNA Conformation. The unexpected finding here was that each of the $A_3 \cdot T_3$ segments had strong concerted propeller twists with positioning of the adenine N-6 amino group so that it forms bifurcated hydrogen bonds to thymine O-4 atoms on two successive thymines. It should be pointed out that this conformation is not found in all six adenine amino groups in the center of the molecule; only four may involve bifurcated hydrogen bonds, and of those only two have favorable geometries that lead us to conclude bifurcated bonds are present. Further interpretation of these results will depend on additional studies that will involve the determination of the position of the hydrogen atoms. Fig. 4 shows a favorable orientation for bifurcated hydrogen bonding. To examine this more carefully, the idealized positions for the hydrogen atoms were generated on the N-6 groups of all of the adenines and the distances and angles between the hydrogens and oxygens were calculated for the base pairs shown in Fig. 4. The distance between the hydrogen on N-6 of A-5 and the oxygen O-4 of T-20 is 2.0 Å, while the distance between the same hydrogen and O-4 of T-19 is 2.1 Å. Furthermore, the angle N-6–H–O-4 is 140° for T-20 and 115° for T-19. This agrees well with the results obtained from an analysis of bifurcated (or three-centered) hydrogen bonds (17). Here we assumed that the N-6 amino groups would remain strictly coplanar with the adenine base, and the N-H bond is 1.0 Å with sp^2 geometry. However, the conformation of the amino groups may be perturbed by the presence of the two electronegative centers in positions quite different from those that are normally found in Watson–Crick base pairs without a strong propeller twist. It is possible that only a relatively small amount of energy is required to rotate the amino group slightly out of the plane of the adenine ring. If this occurs, it will have a considerable effect on the distances between the hydrogen atom and the two oxygen atoms to which it is bonded. This may yield shorter distances for the other potential bifurcating hydrogen bonds in this crystal structure.

It has been known that poly(dA)·poly(dT) melts at a temperature 6°C higher than poly(dA-dT) (3). It is possible that this altered conformation is responsible for the stabilization. In addition, the conformation adopted by fibers of poly(dA)·poly(dT) is rather stable. For example, it does not

form an A-DNA structure upon dehydration (3), nor can it be reconstituted into nucleosomes (5, 6), while poly(dA-dT) is able to undergo both of these conformational changes. Furthermore, poly(dA)·poly(dT) is known to maintain a helical repeat of 10 base pairs per turn in solution (4, 7). A number of models have been proposed for poly(dA)·poly(dT) to account for its anomalous behavior. Alexeev *et al.* (18) have recently proposed an interesting variant of B-DNA with a narrow minor groove and a high propeller twist, but with a large negative base-pair tilt. A similar model has also been proposed by Chuprina (19). Both resemble our model shown in Fig. 5. The major difference between the models is that ours does not have the significant base-pair tilt and the amino groups are therefore in a better position to form bifurcated hydrogen bonds. The model of Alexeev *et al.* (18) has a high propeller twist but the distance between the N-6 of adenine and the O-4 of the thymine (3.6 Å) is too long for a bifurcated hydrogen bond. Our model is also quite different from the heteronomous proposal, which has different conformations in each chain (20).

DNA Bending. The A·T region in our structures is quite straight. There is an overall bending of 11° and 15°, respectively, in the DNA of the drug complex and the DNA alone, and this bending is located mostly at one TG·CA junction. One cannot draw unambiguous conclusions about changes in the helical axis of these DNA dodecamer structures due in part to the fact that all of them have been crystallized in the same lattice in which the DNA molecules are bound together through the last two C·G base pairs. This interaction might distort the bending caused by the sequence itself. If a segment of A·T base pairs in DNA were locked into the structure shown in Fig. 5, there is likely to be a local disruption of the orientation of the helix axis on both sides of the segment relative to the rather straight axis found in the A·T segment. DNA is known to produce bends at sequences in which there are segments of five adenines spaced every 10 base pairs along a DNA helix, such as those found in the small circular DNAs of the trypanosome kinetoplast DNA (21). This bending could arise from the large propeller twist in our poly(dA)·poly(dT) model. An example analogous to this may be seen at the junction of the anticodon stem and the D stem in the three-dimensional structure of yeast phenylalanine tRNA (22). There, a dimethyl N_2 G·A base pair is found with a strong propeller twist. Since the D stem is stacked on one blade of the propeller (m_2^2 G-26) and the anticodon stem is stacked on the opposite side of its paired base (A-44), this produces a bend between the two segments of just over 30°. A similar mechanism might be operating at the ends of these $dA_n \cdot dT_n$ segments, with a smaller bending angle.

The propeller conformation of DNA is unusual: it has stabilizing bifurcated hydrogen bonds in the major groove and a narrow minor groove. The latter might stabilize the spine of hydration. We do not know whether other sequences can adopt this conformation, but it is interesting to note that the N-4 amino group of cytosine-3 also participates in forming a bifurcated hydrogen bond at one end of a $dA_3 \cdot dT_3$ segment. We suggest that this unusual propeller conformation be called P-DNA as a short description of a unique conformation distinct from B-DNA.

It should be pointed out that segments of $dA_n \cdot dT_n$ occur quite frequently in regulatory regions of genes (23, 24). Associated with this has been the recent proposal that DNA may be looped in such a way that it folds back on itself to bring together regulatory proteins that are attached to different segments of the DNA molecule. This looping may be stabilized by $dA_n \cdot dT_n$ segments with large propeller twists. The present structure thus illustrates features that suggest that DNA conformation can vary considerably as a consequence of base sequence and these alternative conformations may be used in a variety of biologically relevant systems.

We wish to thank Dr. G. J. Quigley for helpful discussions and for assistance in various graphic plotting programs and Drs. J. H. van Boom and G. A. van der Marel for supplying the DNA. We also thank Dr. Hillary Nelson for showing her data prior to publication. This work was supported by grants from the National Institutes of Health, the American Cancer Society, the Office of Naval Research. The National Science Foundation and the National Aeronautics and Space Administration. A.H.J.W. also acknowledges support from Burroughs-Wellcome. M.C. is a fellow of the Fulbright Foundation. C.A.F. is a fellow of the Leukemia Society.

1. Zimmer, C. & Wahnert, U. (1986) *Prog. Biophys. Mol. Biol.* **47**, 31–112.
2. Kopka, M. L., Yoon, C., Goodsell, D., Pjura, P. & Dickerson, R. E. (1985) *Proc. Natl. Acad. Sci. USA* **82**, 1376–1380.
3. Arnott, S. & Selsing, E. (1974) *J. Mol. Biol.* **88**, 509–521.
4. Wang, J. C. (1979) *Proc. Natl. Acad. Sci. USA* **76**, 200–203.
5. Simpson, R. T. & Künzler, P. (1979) *Nucleic Acids Res.* **6**, 1387–1415.
6. Rhodes, D. (1979) *Nucleic Acids Res.* **6**, 1805–1816.
7. Rhodes, D. & Klug, A. (1981) *Nature (London)* **292**, 378–380.
8. Wing, R., Drew, H., Takano, T., Broka, C., Tanaka, S., Itakura, K. & Dickerson, R. (1980) *Nature (London)* **287**, 755–758.
9. Hendrickson, W. A. & Konnert, J. (1979) in *Biomolecular Structure, Conformation, Function and Evolution*, ed. Srinvasan, R. (Pergamon, Oxford), pp. 43–57.
10. Jones, T. A. (1978) *J. Appl. Crystallogr.* **11**, 268–272.
11. Nelson, H. C. M., Finch, J. T., Luisi, B. F. & Klug, A. (1987) *Nature (London)*, in press.
12. Behling, R. W. & Kearns, D. R. (1986) *Biochemistry* **25**, 3335–3346.
13. Zakrzewska, K., Lavery, R. & Pullman, B. (1983) *Nucleic Acids Res.* **11**, 8825–8839.
14. Schultz, P. G. & Dervan, P. B. (1984) *J. Biomol. Struct. Dyn.* **1**, 1133–1147.
15. Patel, D. J. (1979) *Eur. J. Biochem.* **99**, 369–379.
16. Klevit, R. E., Wemmer, D. E. & Reid, B. R. (1986) *Biochemistry* **25**, 3296–3303.
17. Taylor, R., Kennard, O. & Versichel, W. (1984) *J. Am. Chem. Soc.* **106**, 244–248.
18. Alexeev, D. G., Lipanov, A. A. & Skuratovski, I. Ya. (1987) *Nature (London)* **325**, 821–823.
19. Chuprina, V. P. (1987) *Nucleic Acids Res.* **15**, 293–311.
20. Arnott, S., Chandrasekaran, R., Hall, I. H. & Puigjaner, L. C. (1983) *Nucleic Acids Res.* **11**, 4141–4155.
21. Marini, J. C., Levene, S. D., Crothers, D. M. & Englund, P. T. (1982) *Proc. Natl. Acad. Sci. USA* **79**, 7664–7668.
22. Kim, S. H., Suddath, F. L., Quigley, G. J., McPherson, A., Sussman, J. L., Wang, A. H.-J., Seeman, N. C. & Rich, A. (1974) *Science* **185**, 435–440.
23. Bossi, L. & Smith, D. M. (1984) *Cell* **39**, 643–652.
24. Widom, J. (1985) *BioEssays* **2**, 11–14.